Effect of Alkali Atom Doping on the Electronic Structure and Aromatic Character of Planar and Quasi-Planar Al13+ Clusters

Surajit Guin
Behala College
Atish Dipankar Jana (atishdipankarjana@yahoo.in)
Behala College https://orcid.org/0000-0003-1364-1360

Research Article

Keywords: Pure planar/quasi-planar aluminium cluster, Alkali doped Al13+ cluster, ESP surface, Canonical Molecular Orbital: HOMO and LUMO, NICS analysis, LOL analysis, ELF analysis

Posted Date: March 10th, 2021

DOI: https://doi.org/10.21203/rs.3.rs-245868/v1

Version of Record: A version of this preprint was published at Journal of Molecular Modeling on August 1st, 2021. See the published version at https://doi.org/10.1007/s00894-021-04845-7.

Abstract

A set of three Al_{13}^+ clusters, one perfectly planar and two quasi-planar structures have been recently reported by our group [Guin et. al. Journal of Molecular Graphics and Modeling, 2020, 97, 107544]. One of the quasi-planar structures is true minima (GS) with zero imaginary frequency and another one is transition state structure (TS) with one imaginary frequency, whereas the perfectly planar structure has three imaginary frequencies. All three posses bilaterally symmetry with identical structural features - a set of ten aluminium atoms encircle a triangular core and also this set of three aluminium cluster is a rare example of a metallo-aromatic system in which highly anti-aromatic islands are embedded in an aromatic sea. One of the atoms of the central triangle lies on the symmetry axis and is crucial for the stability of these clusters. In the present study, we have explored the effect of doping alkali atoms (Li, Na and K) at this pivotal site of the cluster with an aim to understand the structural stability and the effect on the aromatic character as compared to the parent clusters. Besides the electronic structural analysis, NICS and ELF studies have also been carried out to characterize the aromatic nature of the doped clusters. Interestingly it has been found that even with the incorporation of the alkali atoms the bilateral symmetry of the clusters remains intact but instead of the central position the alkali atoms drift towards the periphery of the cluster along the symmetry line and equilibrate on the periphery. The dipole moment of the clusters systematically increases and the overall aromaticity of the cluster systematically decreases with the increase in the atomic number of the dopant alkali atoms.

Introduction

During current times, nano-clusters, as well as doped nano-clusters have drawn inquisitive attention of scientists due to their versatile properties and potential applicability in various fields like optics[1], electronics[2], catalysis[3], sensors[4] etc. Nano-clusters quite often exhibit unanticipated properties which are vastly different from their bulk counterpart. Especially, doped metal nano-clusters have additional advantages compared to the undoped clusters as this brings out the opportunity to amalgamate properties of different metal atoms into a single entity. Studies of these nano-clusters also provide deeper understanding regarding the origin of stability as well as different possible isomers due to various geometric configurations [5]. Among various metal nano-clusters, aluminium nano-clusters have been found to have a wide range of applications in various fields like catalysis[6], storage of hydrogen[7], splitting of water to produce hydrogen[8] etc. Aluminium is a cheaper material due to its higher natural abundance as well as the ease with which it can be tailored in various architectures like nano-rods[9], nano-disks[10] and nano-shells[11]. Recently Jiang et al. have reported various structural possibilities for Al_mB_m (n=1-7 and m=1-2) using [12]. Q. L. Lu et al have reported the cage-like structure of Al_{12} by DFT calculation which has revealed that the presence of Mg, Ca metals enhance the stability of the aluminium cluster significantly[13]. In 2017, Li et al. investigated geometries, stabilities and electronic properties palladium doped aluminium clusters having general formula Al_nPd_m (n=1-10,m=1,2) by using DFT calculation[14]. In 2017, Jia et al have reported low lying isomers of Al_nAs_q (q=-1,0,+1;n=1-16) [15].

Here in the current paper, we report the effect of doping of alkali atoms Li, Na and K at the core of the recently reported planar and quasi-planar Al_{13}^+ clusters by our group [16, 17]. It was found that Al_{13}^+ cluster can exist in three closely lying isomeric form, a perfectly planar cluster, and two quasi-planar clusters, slightly puckered in opposite direction with respect to the planar cluster. Among these two quasi-planar clusters one is a true minimum structure (GS) and the other one is a transition state (TS). This ground state (GS) structure was found to be more aromatic compared to the planar and TS structure. These clusters have a common structural feature - in each of these a triangular core is encircled by a set of ten aluminium atoms (Fig 1a). These clusters all posses a bilateral symmetry which readily passes through this central triangular core bisecting it with one of the Al atoms lying on the symmetry line. It was found that the stability of these clusters is crucially dependent on this Al atom that lies on the symmetry line. The aim of the current study is to explore the effect of alkali atom doping at the position of this Al atom. It is quite interesting that bilateral symmetry is a robust feature of this system which is maintained even after alkali atom doping. Also, the alkali atoms prefer the peripheral position in the cluster even if the doping is done at the bulk position at the core of the cluster. Detailed electronic structure analysis of these doped clusters has revealed the origin of structural rearrangement due to doping. Nucleus Independent Chemical Shift (NICS), which is an efficient aromaticity indicates that aromatic nature of Al_{13}^+ cluster changes to anti-aromatic cluster due to overall loss aromaticity index has been computed for these clusters which reveal that alkali doping reduces the aromatic character of the system. Electron Localization Function (ELF) which is also a modern tool in theoretical chemistry to characterize aromaticity has provided insight into the nature of aromaticity of these doped systems. This study has also revealed that alkali atom doping can be effectively utilized to systematically tune the dipolar nature of these clusters.

Computational Methodology

Gaussian 03 package[18] has been employed to explore the optimized geometry of alkali doped Al_{13}^+ clusters using the DFT methodology employing the B3LYP hybrid density functional. 6-311G(d) basis set [19]. Threshold values of convergence criterion in the optimization process for maximum force and displacement are 0.000450 a.u. and 0.001800 a.u. respectively whereas that for the RMS force and displacement are 0.000300 a.u. and 0.001200 a.u. respectively [20]. Once the current values of all four criteria fell below the threshold, the nature of the optimized structures were characterized by frequency analysis. All quasi-planar structures correspond to true minimum structure with zero imaginary frequency. Graphics for canonical orbitals and electrostatic potential (ESP) [21] were generated using Molekel[22] and Chemissian package[23] whereas ELF analysis has been carried out using Multiwfn-3.7 package[24]. NICS(0) values have been computed using Gaussian 03 package.

Results

A set of three planer as well as quasi-planar Al_{13}^+ clusters with interesting metallo-aromatic properties have been recently reported by our group. In all of these clusters, a central triangular core is encircled by a

set of ten Al atoms in the form of a belt (Fig. 1(a)). Also, these clusters have a unique commonality – all of these possess a bilateral symmetry with respect to a symmetry line that passes through the middle of the cluster bisecting the central triangular core with one of the Al atoms situated on this symmetry line. Besides bonding to two other atoms at the core, this particular Al atom also establishes bonding with three other Al atoms on the periphery of the cluster which is also crucial for the stability of the cluster. The present study aims to understand the effect of doping alkali atoms Li, Na and K right at the position of this crucial point of stability replacing the central Al(1) atom. In the process of searching the optimized structures in the presence of doped alkali atoms, besides the quasi-planar true minimum structure characterized by the presence of zero imaginary frequency in the vibrational analysis of the structure we have also obtained planar Li, Na and K doped Al_{13}^+ clusters having 3, 3 and 6 imaginary frequencies respectively. The electronic structures of these planar structures have been explored along with the quasi-planar minimum energy structures to understand the nature of the distortion and the effect on aromaticity as the clusters evolve from planar to the quasi-planar puckered structures.

Optimized geometries of alkali atom (Li, Na and K) doped Al_{13}^+ clusters have been depicted in Fig. 1. It is to be noted that, previously reported planar and quasi-planar Al_{13}^+ clusters possess a bilateral symmetry (Fig. 1a). The doping of alkali atoms at the position of Al(1) does not destroy this bilateral symmetry; rather, the alkali atoms occupy their positions on this symmetry line. In case of planar clusters (which are not true minimum structures) the alkali atoms remain within the bulk of the cluster but for the quasi-planar true minimum structures the alkali atoms occupy the peripheral position on the symmetry line (Fig 1(b), Fig 1(c), Fig 1(d)).

In case of Li doping, lower part of the cluster is affected most, the upper portion remains nearly undistorted. Two rhombic grids at the middle of the planar Al_{13}^+ clusters are diagonally joined by the effect of the Li atom at position 1 which establish two shorter bonds Li(1)-Al(6) = 2.929 Å and Li(1)-Al(12) = 2.929 Å as compared to 2.736 Å between Al(1)-Al(3) and Al(1)-Al(2) in the undoped planar Al_{13}^+ cluster. Atoms Al(13) and Al(5) go away from the position of atom 1 which give rise to two approximate rectangular grids at the lower half of the cluster. The Li(1) – Al(4) distance is 2.665 Å which is smaller compared to Al(1) -Al(4) distance (2.714 Å).

On the other hand, the central triangle is also reformed maintaining its symmetry with Li(1)-Al(2) = 2.643 Å and Li(1)-Al(3) =2.643 Å as compared to 2.736 Å between Al(1)-Al(3) and Al(1)-Al(2) in the undoped planar Al_{13}^+ cluster. Even this effect of doping of lighter atom at position 1 also reduces bond distance among Al(2)-Al(3) {2.567 Å from 2.736 Å}. A pair of square at the bottom surface of the cluster has been formed due to doping. But geometry of top region of the cluster remains same. Maximum horizontal and vertical dimension ratio in this case is 7.930 Å: 7.408 Å.

The minimum energy quasi-planar structure corresponding to the centrally Li doped planar cluster has been depicted in the lower panel of Fig 1(b). It is interesting to note that, now the Li atom has swapped its position with Al(4) which was at the periphery of the pure Al_{13}^+ clusters. This effect is a generic feature

and is observed in case of Na and K doping as well (Fig 1(c) and Fig 1(d)). Alkali atoms prefer to occupy the peripheral position compared to a bulk one. A comparison of the Li doped true minimum structure with the corresponding quasi-planar Al_{13}^+ shows that now not only the lower part of the cluster but all thirteen atoms of the cluster readjusts itself and Li doped cluster is more puckered compared to the quasi-planar Al_{13}^+cluster. In this puckered configuration the cluster assumes a flying bird like shape with two symmetry related edges (formed by Al(5), Al(6), Al(7) and their symmetry related Al(13), Al(12) and Al(11)) analogous to two wings, Li(1) which is placed slightly downwards of the mean plane forms the tail and three aluminium aotms (Al(8), Al(9) and Al(10)) at the upper edge form the head portion of the cluster. An account of the bond distances and dihedral angles between adjacent triangular rings of the cluster have been provided in table 1and table 2 respectively.

In case of Na doped Al_{13}^+ cluster, doping of Na atom at position 1 enlarges the bond distance among Na(1)-Al(2)/Al(3) { 2.953 Å from 2.736 Å }.This effect of doping also enhances the bond distance among Al(2)-Al(3) {2.857 Å from 2.736 Å}. Due to presence of Na atom at position 1, Al(4) is displaced more downward and knocked out from the bond connected by Na(1), Al(5) and Al(13). The bilateral symmetry along y-axis remains intact even in the presence of Na. Maximum horizontal and vertical dimension extension of the cluster in this case is 8.082 Å and 8.460 Å. Bond distances and bond angles for the cluster has been summarized in table S1.

In the true minima Na doped quasi-planar structure, Na(1) and Al(4) swap their locations along the symmetry line. Also Na(1) atom is located 2.46Å downward of the mean plane passing through the central Al_3 triangular core. Aluminium atoms Al(5), Al(6) and Al(7) on the left edge, as well as their symmetry related counterparts Al(13), Al(12) and Al(11) moves upward 0.54 Å, 1.95 Å and 1.52 Å respectively) of the mean plane passing through the central triangular core. This give rise to a puckered geometry of the cluster rendering the cluster a shape analogous to a flying bird with Na(1) occupying the tail region and three aluminium atoms Al(8), Al(9) and Al(10) forming the head portion of the cluster. Al(9) is placed slightly upward (0.43 Å) of the mean plane passing through the central triangular core.

In case of K doping also, both the planar and the quasi-planar clusters have the analogous topologies like those of the Na doped cluster. In case of the planar cluster K(1)-Al(4) distance is relatively longer compared to Li and Na doped clusters. Bond distances K(1)-Al(2)/Al(3) (3.116 Å) is much longer than the corresponding distance of parent Al_{13}^+ cluster (2.736 Å). This effect of doping slightly increases the bond distance among Al(2)-Al(3) {2.927 Å from 2.736 Å}also. Maximum horizontal and vertical dimension of the cluster in this case is 8.159 Å: 7.783 Å.

The true minima K doped quasi-planar cluster has a similar bird like architecture as that was found in case of Li and Na doped cluster. The geometrical parameters (bond distances, bond angles and dihedral angles between adjacent rings) have been provided in table 1. Both the planar and quasi-planar K doped clusters posses bilateral symmetry along y-axis.

Among the three quasi-planar Li, Na and K doped clusters; the major differences prevail around the tail region. Dopant alkali atoms are displaced downwards with respect to the mean plane passing through the central triangular core constituted by Al2, Al3 and Al4 (Fig. 2). Figure 2 depicts the superposed view of the three alkali doped clusters in which the alignment has been done with Al4 as origin, y-axis passing thorough origin and the middle of the arm formed by Al2 and Al3, x - axis was taken parallel to this arm and z = 0 was set for the plane passing this triangle. From figure 2(b) it can be seen that the distance of the alkali atoms from the origin (position of Al4) increases in accordance with the increasing atomic number of the alkali atoms. K is displaced downward highest (2.62Å) from the mean plane, Na has an intermediate downward displacement (2.46Å) and Li has the least (2.35Å) downward displacement among the three alkali atoms. The distances of the projection points of K, Na and Li on the symmetry axis (y-axis) from Al4 (which is at origin) are 2.32 Å, 1.75 Å and 1.30 Å respectively. As can be seen from figure 2, the central triangular core for all three clusters is almost identical. From figure 2(b) it is also evident that the upper part of the clusters (consisting of peripheral Al6, Al7, Al8, Al9, Al10, Al11and Al12) deviate upward of the mean plane. Al5 and symmetry related Al13 deviate downward of the mean plane. The magnitude of the upward deviation of the Al atoms at the upper portion of the cluster is maximum for Li-doped cluster, intermediate for Na-doped cluster and least for Li-doped cluster whereas for the lower portion of the cluster this sequence is reversed, K-doped cluster has the maximum downward deviation, Li-doped cluster has the lowest downward deviation and Na-doped cluster has intermediate value (see Fig 2a). For all three clusters, the upward deviation for Al7 and symmetry related Al11 are practically the same.

Table 1: Geometrical parameter of the quasi-planar Li, Na and K doping Al_{13}^{+} clusters

	Li doping	Na doping	K doping
	Bond distances (Å)		
Bonds	**Inner triangular core**	**Inner triangular core**	**Inner triangular core**
4-2	2.653	2.657	2.666
4-3	2.653	2.657	2.666
2-3	2.670	2.763	2.749
	Core-periphery	**Core-periphery**	**Core-periphery**
2-7	2.865	2.866	2.897
2-8	2.937	2.907	2.903
2-6	2.712	2.730	2.725
2-9	2.718	2.717	2.714
3-10	2.937	2.906	2.902
3-11	2.865	2.886	2.897
3-9	2.718	2.717	2.714
3-12	2.712	2.730	2.726
4-5	2.604	2.611	2.594
4-13	2.604	2.611	2.594
4-1	2.683	3.015	3.495
	Intra periphery	**Intra periphery**	**Intra periphery**
1-5	2.900	3.310	3.793
13-1	2.900	3.310	3.793
5-6	2.495	2.502	2.508
13-12	2.495	2.502	2.508
6-7	2.615	2.605	2.601
12-11	2.615	2.605	2.601
7-8	2.502	2.524	2.523
11-10	2.524	2.524	2.523
8-9	2.622	2.622	2.621

10-9	2.622	2.622	2.621
	Core bond angles(˚)		
2-4-3	58.12	62.68	62.07
4-2-3	60.94	58.66	58.96
2-3-4	60.94	58.66	58.96

Table 2: Dihedral angles of quasi-planar Li, Na and K doping Al_{13}^{+} clusters, for planar clusters corresponding dihedral angles are 180° each.

Dihedral angle between	Value of dihedral angle		
	Li doping	Na doping	K doping
R1-R8	48.13°	42.04°	36.79°
R1-R3	26.99°	21.56°	17.35°
R2-R2*	16.97°	15.94°	14.44°
R2-R3	46.55°	42.95°	39.32°
R3-R4	74.71°	73.91°	71.13°
R4-R5	7.69°	12.46	15.05°
R5-R6	30.19°	29.73°	29.21°
R6-R7	92.28°	92.75°	92.42°
R7-R8	34.02°	32.76°	32.42°

The dihedral angle between the central ring (R1) and the adjacent ring (R8) on top of the cluster is 48.13°, 42.04° and 36.79° respectively for the Li, Na and K doped clusters. The highest dihedral angle is between R6 and R7 which is the (92.28°, 92.75° and 92.42° for Li, Na and K doped clusters) highest and this leads to maximum puckering at the upper left and upper right corner of the clusters. Next highest puckering is between the ring R3 and R4 and the least puckering is between the rings R4 and R5 (Table 2). This deviation leads to the architecture of the cluster analogous to the upwardly displacement of two wings of a flying bird.

Table 3: Dipole moments of clusters

Cluster	Planar/ Quasiplanar	Dipole Moments in Debye			
		μ_x	μ_y	μ_z	$\|\mu\|$
Pure Al	Planar	-0.0000018	-0.3812093	0.000000	0.38
	True minima	0.0000584	-0.4487331	0.0974657	0.45
Li doped	Planar	0.0002488	-1.807476	0.000000	1.81
	True minima	0.0024805	-1.3447913	-0.9533147	1.64
Na doped	Planar	0.0003463	-2.4938611	0.000000	2.49
	True minima	0.0037028	-1.9788788	-1.3849868	2.40
K doped	Planar	0.0004881	-1.6697678	0.000000	1.67
	True minima	0.0054952	-3.0122418	-2.1733071	3.70

ESP surface of alkali doped Al_{13}^+ cluster has been depicted in Fig. 3. Dipole moment [25] of these clusters has been provided in table 3. In the Li doped cluster, Li(1) is the most electron rich region (red) throughout the whole cluster, whereas electron deficit regions (indicated by blue color) is spread over the periphery of the cluster. The net dipole moment of the cluster is aligned along symmetry axis (y-axis) of the cluster (-1.81 Debye). The x-component of the dipole moment has a negligible value. For Li doped qusi-planar structure, there is significant z-component of dipole moment (-0.95 Debye), but the net dipole moment for this cluster is (-1.64 Debye) which is slightly less than the planar counterpart.

In case of Na doped planar cluster, Na(1) is the most electron rich region (red) within the whole cluster, whereas electron deficit region is spread over the whole periphery of the cluster. In this case the net dipole moment of the cluster is aligned along negative y-axis (along symmetry line) of the cluster (-2.49 Debye). The x and z component of dipole moments have negligible values. For Na doped quasi-planar cluster the z-component of dipole moment and the total dipole moment values are respectively 1.38 Deby and 2.40 Debye.

For the K doped cluster, the most electron concentration occur around the K(1) atom the centre of the cluster. Upper left (comprising of Al(7) and Al(8)) and upper right (comprising of Al(10) and Al(11)) corners of the cluster are the electron deficit regions. Rest of the other region of the cluster has intermediate electron density. Net dipole moment of the cluster is aligned along the symmetry line of the cluster (y-axis) and has a value -1.67 Debye. For the corresponding quasi-planar cluster the z-component of dipole moment and the net dipole moment values are respectively 2.71Deby and 3.70 Debye respectively.

The dipole moment of the clusters systematically increases with the atomic number of the dopant alkali atoms. For the quasi-planar clusters, going from Li to Na to K doping, the dipole moment increases from 1.64 Debye to 2.40 Debye to 3.70 Debye. This trend in the systematic increase in the dipolemoment

vlaues can be understood from the fact theat he higher atomic number alkali atoms are easily polarizable due to their soft nature. So, the present system is possibly a unique one where the dipole of the cluster can be tuned by doping alkali atom of various sizes keeping the direction of the dipole fixed. Also it is to be noted that whereas in the pure Al_{13}^{+} cluster the net dipole moment value is quite small (0.45 Deby), the doping of alkali atoms can increase the polarity of the system by an order of magnitude.

Canonical Molecular Orbitals

A scrutiny of the nature of the molecular orbitals provides important information such as electron delocalization and molecular reactivity [26]. Delocalized electronic orbitals are directly related to the aromatic/anti-aromatic character of a system. Energy difference between Highest Occupied Molecular Orbital (HOMO) and Lowest Unoccupied Molecular Orbital (LUMO) of a cluster is correlated with the reactivity of the cluster. Lower HOMO-LUMO gap clusters are expected to be more reactive in nature. Fig 4 depicts the HOMO-LUMO orbitals and the HOMO-LUMO gap for all the clusters.

For pure Al_{13}^{+} cluster, HOMO has substantially delocalization due to π-electrons and LUMO has significantly delocalization due to purely σ-electrons for planar structure and for quasi-planar structure it is π character. HOMO-LUMO gap for the planar cluster is 1.583 eV and for the quasi-planar cluster, it is 1.373 eV. For Li doped cluster, HOMO and LUMO both have substantially delocalization due to π-electron and σ-electron respectively for planar and the quasi-planar structure as well. In this case, the HOMO-LUMO energy gap is 0.536 eV and 1.251 eV respectively for planar and quasi-planar structures. For Na doped Al_{13}^{+} cluster, the situation is a little bit different. Here, in both cases, HOMO has substantially delocalization due to σ-electron, but LUMO has significantly delocalization due to purely π -electrons. In this case, HOMO-LUMO gap energy is 0.386 eV and 1.231 eV respectively for planar and quasi-planar structures. For K doped Al_{13}^{+} cluster, HOMO has substantially delocalization due to π-electrons and LUMO has significantly delocalization due to purely σ-electrons. For quasi-planar structure both are σ characters. In this case, the HOMO-LUMO gap is 0.83 eV and 1.331 eV respectively for planar and quasi-planar structures.

From the HOMO-LUMO gap values it is clear that for pure quasi-planar Al_{13}^{+} cluster the gap is higher (1.373 eV) compared to the alkali doped clusters, among which Na doping leads to the highest reduction in the energy gap value (to 1.231 eV). So, the doping of alkali atom at the core, tend to reduce the energy gap of the cluster. It is interesting to note that energy gap values are in the semiconducting region which is tunable through the doping by alkali atoms.

Nucleus Independent Chemical Shift (NICS) analysis:

Nucleus independent chemical shift (NICS) is the widely used magnetic criterion of aromaticity [27]. A high negative value of NICS indicates the aromatic character of a ring, a high positive value of NICS indicates anti-aromatic character, whereas a small value of NICS indicates the non-aromatic nature of a ring. NICS(0) is the value of NICS computed at the ring plane at z = 0Å height at the centroid of a ring.

As shown in Fig 5, each cluster consists of fourteen triangular sub-regions. NICS(0) values have been computed at the centroid of each of these triangles. As each structure has bilateral symmetry, the symmetry-related triangles located on the right-hand part of the clusters have the same NICS(0) values as that of the left-hand part. As can be seen from Fig 5, at the centre of the planar and quasi-planar pure Al_{13}^+ clusters the NICS(0) values are respectively -5.82 ppm and -4.40 ppm. Corresponding NICS(0) values for the planar Li, Na and K doped clusters are respectively +18.57ppm, +25.73ppm and +38.97ppm indicating a strong anti-aromatic at the core of the planar clusters. On the other hand, in the case of quasi-planar clusters the NICS(0) values at the centre of ring R1 are respectively 2.81ppm, -1.44ppm and 2.22ppm for the Li, Na and K doped clusters. This data reveals that doping of alkali metal induces anti-aromatic character of the central ring which relaxes to corresponding quasi-planar cluster by shedding anti-aromaticity. Rings at the upper left (R5, R6, R7, R8) and upper right corners (R5*, R6*, R7*, R8*) of the pure planar and quasi-planar Al_{13}^+ clusters are having quite a high negative NICS(0) values at the centre of these rings. Among these, ring R6 has the highest negative NICS(0) value. For planar Al_{13}^+ this value is -18.03ppm and for the quasi-planar, it is -18.02 ppm. For the doped quasi-planar clusters on the other hand the highest negative NICS(0) occur at the centre of ring R7. For the Li doped cluster, this value is -11.50ppm, for the Na doped cluster -9.88ppm and for the K doped cluster, the value is -10.74ppm. So even in the doped clusters, the top portion of the cluster retains substantial aromaticity. In summary, the effect of alkali atom doping is to reduce the aromaticity with respect to the parent cluster.

Electron Localization Function (ELF) analysis:

Electron localization function (ELF) is a dimensionless quantity and its value varies between zero and one [28]. The closer the value of ELF is to one, the lower is the probability of an electron of a particular spin to be present near another electron of the same spin at an arbitrary position r. A lower value of ELF indicates a higher level of electron localization and a higher value indicates electron delocalization. Analysis of electron localization function provides clues to the presence or absence of aromaticity in a chemical system. Continuity of the ELF iso-surface at least at an iso-value of 0.70 is assumed to be the acceptability criterion for the existence of aromaticity in a chemical system. As one increases the iso-value from 0.70 towards 1.00, at a certain iso-value the continuity of ELF iso-surface appears to break and these are known as the bifurcation points. The higher is the iso-value at which the bifurcation occurs in a chemical system, the higher is the electron delocalization and also the aromatic nature of the system.

The study of the electron localization function (ELF) and its bifurcation points for the quasiplanar Al_{13}^+ clusters have been compared with the alkali doped clusters in Fig. 6. The total electron localization function of the quasi-planar Al_{13}^+ cluster shows that at an iso-value of 0.70 the ELF surface consists of two distinct islands spread over the periphery of the cluster. There is also a visible delocalization over the triangular core of the cluster. In the case of alkali doped clusters, the continuity of iso-surface is spread over the aluminium atoms and the alkali atoms are separately enclosed by a distinct spherical iso-surface. The electron delocalization in this case has a total continuity over the whole periphery traced through the Al atoms excluding the alkali atoms at the lower tip of the cluster. It is to be noted that there

is also an electron delocalization over the triangular core of the doped clusters which is in 'Y' shape and this connects the core region to the peripheral delocalized iso-surface. In the case of the Li doped cluster at an iso-value of 0.70, this core delocalization ('Y') is slightly more elongated compared to the Na and K doped clusters. At an iso-value of 0.75, the parent Al_{13}^+ cluster has three distinct islands over the periphery and the delocalization over the core of the cluster is detached from the periphery. At this iso-value, in the case of the Li doped cluster, there is a bifurcation at the lower end of the periphery and the central delocalization is also separated from the peripheral delocalization. In the case of Na and K doped clusters though the peripheral delocalization is maintained even at this iso-value the core delocalization just gets detached from the peripheral delocalization. In the case of the K doped cluster, the peripheral delocalization is more dominant compared to the Na doped cluster. At an iso-value of 0.80, the parent Al_{13}^+ cluster still retains the three distinct delocalized regions at the upper left, upper right and the lower tip of the cluster with a reduced spread of the iso-surface. But at 0.80 iso-value for the Li doped cluster, there is complete detachment of the iso-surface through peripheral bifurcations at the top left and top right corner of the cluster, which appears to be setting in for Na and K doped clusters. At an iso-value of 0.85 there are six distinct separated iso-surfaces over the periphery for the Li doped cluster, but four distinct iso-surfaces in the case of Na and K doped clusters. At an iso value of 0.90 there is no continuity of the iso-surfaces left over the periphery for any of the clusters. This study indicates that alkali atoms do not cooperate with Al atoms in electron delocalization. Aluminium atoms over the periphery and the triangular core have distinct delocalization. The peripheral delocalization appears to be stronger compared to that at the core. In the presence of alkali atoms, the peripheral delocalization among the nine aluminium atoms become stronger compared to the ten aluminium atoms of the parent Al_{13}^+ cluster. The alkali atoms though are not directly part of this delocalized iso-surfaces, surely influence the cooperativity among the aluminum atoms themselves, the strength of influence increasing in the sequence Li, Na and K. Alkali atoms thus act as foreign attackers which and catalyzes the cooperativity among the aluminium atoms themselves.

Conclusion

In summary, we have explored in detail the effect of doping alkali atoms Li, Na and K at the core of both planar and quasi-planar minimum energy Al_{13}^+ clusters. There are quite a few interesting findings regarding alkali doped clusters. First of all, even in the presence of doped alkali atoms, the clusters retain bilateral symmetry. So the bilateral symmetry is a robust feature of the Al_{13}^+ and its alkali doped counterparts. The second interesting observation is that the polarity of the clusters increase substantially (nearly ten times) with respect to the pure Al_{13}^+ cluster when alkali atoms of a higher atomic number are doped. In all cases, the dipole moment is directed along the symmetry axis of the cluster. The third interesting observation is that the alkali atoms prefer the peripheral positions instead of the central position which facilitates energy minimization. So, aluminium atoms try to remain together through homo-philicity and dopant atoms are pushed towards the edge of the cluster in such a way that the cluster tends to maintain the inherent bilateral symmetry. The HOMO-LUMO energy gap tends to reduce in

the presence of alkali atoms, which all fall in the semiconducting region. NICS(0) results show that alkali doping tends to reduce the aromatic character of the cluster compared to the undoped parent cluster. ELF study indicates that electron delocalization and cooperativity among the aluminium atoms is increased in the presence of alkali atoms in the sequence Li, Na and K. Finally, metal nano-clusters, which have found many potential technological applications, are attracting the attention of the scientific community due to their tunability both by controlling shape and size. The present study has revealed that the polarity of the HOMO-LUMO energy gap of planar and quasi-planar Al_{13}^{+} clusters are tunable through doping alkali atoms which should find an application of this cluster in the field of nano-electronics.

Declarations

Funding: A. D. J. acknowledges the financial support from the Department of Science, Technology and Biotechnology, Government of West Bengal, India through the project memo no: 250(Sanc.)/ST/P/S&T/16G-47/2017 Date: 25/03/2018. S. Guin acknowledges financial support from the UGC India for JRF fellowship ref no 1432/(CSIR-UGC NET DEC-2018).

Conflict of interest/Competing interests: There is no conflict of interest between the authors

Availability of data and material: N/A

Code Availability: N/A

Author's contributions: S. Guin is responsible for computational works, A. D. Jana is contributed by conceptualizing the problem and writing the manuscript.

References

1. Mandal S, Wang J, Winans RE, et al (2013) Quantum size effects in the optical properties of ligand stabilized aluminum nanoclusters. J Phys Chem C 117:6741–6746. https://doi.org/10.1021/jp310514z
2. Qingfeng Tan , Xiaojun Bao , Tengchun Song , Yu Fanb, Gang Shi , Baojian Shen ,Conghua Liu , Xionghou GaoJournal of Catalysis 251 (2007) 69–79 (2016) Synthesis, characterization, and catalytic properties of hydrothermally stable macro–meso–micro-porous composite materials synthesized via in situ assembly of preformed zeolite Y nanoclusters on kaolin doi:10.1016/j.jcat.2007.07.014
3. Tan Q, Bao X, Song T, et al (2007) Synthesis, characterization, and catalytic properties of hydrothermally stable macro-meso-micro-porous composite materials synthesized via in situ assembly of preformed zeolite Y nanoclusters on kaolin. J Catal 251:69–79. https://doi.org/10.1016/j.jcat.2007.07.014
4. King NS, Liu L, Yang X, et al (2015) Fano Resonant Aluminum Nanoclusters for Plasmonic Colorimetric Sensing. ACS Nano 9:10628–10636. https://doi.org/10.1021/acsnano.5b04864

5. Li YF, Zhang FQ, Ren FQ, Ma WJ (2018) Geometries, stabilities and electronic properties of bimetallic AlnPdm (n = 1-10, m = 1; 2) clusters. Int J Mod Phys B 32:1–13. https://doi.org/10.1142/S021797921850073X
6. Knözinger H, Ratnasamy P (1978) Catalysis Reviews: Science and Engineering Catalytic Aluminas: Surface Models and Characterization of. Catal Rev 31–70. https://doi.org/10.1080/03602457808080878
7. Maatallah M, Guo M, Cherqaoui D, et al (2013) Aluminium clusters for molecular hydrogen storage and the corresponding alanes as fuel alternatives: A structural and energetic analysis. Int J Hydrogen Energy 38:5758–5767. https://doi.org/10.1016/j.ijhydene.2013.03.015
8. Dupiano P, Stamatis D, Dreizin EL (2011) Hydrogen production by reacting water with mechanically milled composite aluminum-metal oxide powders. Int J Hydrogen Energy 36:4781–4791. https://doi.org/10.1016/j.ijhydene.2011.01.062
9. Mamat MH, Khusaimi Z, Musa MZ, et al (2011) Fabrication of ultraviolet photoconductive sensor using a novel aluminium-doped zinc oxide nanorod-nanoflake network thin film prepared via ultrasonic-assisted sol-gel and immersion methods. Sensors Actuators, A Phys 171:241–247. https://doi.org/10.1016/j.sna.2011.07.002
10. Martin J, Plain J (2015) Fabrication of aluminium nanostructures for plasmonics. J Phys D Appl Phys 48:184002. https://doi.org/10.1088/0022-3727/48/18/184002
11. Hirsch LR, Gobin AM, Lowery AR, et al (2006) Metal nanoshells. Ann Biomed Eng 34:15–22. https://doi.org/10.1007/s10439-005-9001-8
12. Ahmed F, Ghosh SR, Halder S, et al (2019) Metal-ligand ring aromaticity in a 2D coordination polymer used as a photosensitive electronic device. New J Chem 43:2710–2717. https://doi.org/10.1039/C8NJ05526B
13. Gerard D, Gray SK (2015) Aluminium plasmonics. J Phys D Appl Phys 48:184001. https://doi.org/10.1088/0022-3727/48/18/184001
14. Ooi KJA, Ang YS, Zhai Q, et al (2019) Nonlinear plasmonics of three-dimensional Dirac semimetals. APL Photonics 4:. https://doi.org/10.1063/1.5042450
15. Loyez M, Larrieu JC, Chevineau S, et al (2019) In situ cancer diagnosis through online plasmonics. Biosens Bioelectron 131:104–112. https://doi.org/10.1016/j.bios.2019.01.062
16. Guin S, Ghosh SR, Jana AD (2020) Planarity does not always mean higher aromaticity – Intriguing metalloaromaticity of three Al13+ isomers. J Mol Graph Model 97:107544. https://doi.org/10.1016/j.jmgm.2020.107544
17. Guin S, Ghosh SR, Jana AD (2018) First report of a planar and a quasi-planar Al13+ cluster having localized antiaromatic deltas within an aromatic sea: NICS, ELF, AIM, and AdNDP bonding analysis. J Mol Model 24:1–14. https://doi.org/10.1007/s00894-018-3875-5
18. M.J. Frisch, G.W. Trucks, H.B. Schlegel, G.E. Scuseria, M.A. Robb, J.R. Cheeseman, J.J.A. Montgomery, T. Vreven, K.N. Kudin, J.C. Burant, J.M. Millam, S.S. Iyengar, J. Tomasi, V. Barone, B. Mennucci, M. Cossi, G. Scalmani, N. Rega, G.A. Petersson, H. Nakatsuji, M. Hada, M. Ehara, K. Toyota,

R. Fukuda, J. Hasegawa, M. Ishida, T. Nakajima, Y. Honda, O. Kitao, H. Nakai, M. Klene, X. Li, J.E. Knox, H.P. Hratchian, J.B. Cross, C. Adamo, J. Jaramillo, R. Gomperts, R.E. Stratmann, O. Yazyev, A.J. Austin, R. Cammi, C. Pomelli, J.W. Ochterski, P.Y. Ayala, K. Morokuma, G.A. Voth, P. Salvador, J.J. Dannenberg, V.G. Zakrzewski, S. Dapprich, A.D. Daniels, M.C. Strain, O. Farkas, D.K. Malick, A.D. Rabuck, K. Raghavachari, J.B. Foresman, J.V. Ortiz, Q. Cui, A.G. Baboul, S. Clifford, J. Cioslowski, B.B. Stefanov, G. Liu, A. Liashenko, P. Piskorz, I. Komaromi, R.L. Martin, D.J. Fox, T. Keith, M.A. Al-Laham, C.Y. Peng, A. Nanayakkara, M. Challacomb, P.M.W. Gill, B. Johnson, W. Chen, M.W.Wong, C. Gonzalez, J.A. Pople, Gaussian 03, Revision C.02, Gaussian, Inc, Wallingford CT, 2004.

19. Salasco L, Dovesi R, Orlando R, et al (1991) A periodic ab initio extended basis set study of A-Al203. Mol Phys 72:267–277. https://doi.org/10.1080/00268979100100201
20. Yuan G, Rogers ETF, Zheludev NI (2019) “Plasmonics” in free space: observation of giant wavevectors, vortices, and energy backflow in superoscillatory optical fields. Light Sci Appl 8:. https://doi.org/10.1038/s41377-018-0112-z
21. Weiner PK, Langridge R, Blaney JM, et al (1982) Electrostatic potential molecular surfaces. Proc Natl Acad Sci U S A 79:3754–3758. https://doi.org/10.1073/pnas.79.12.3754
22. S. Portman, P.H. Lüthi, MOLKEL: an interactive molecular graphics tool, Chimia 54 (2000) 76333
23. Heard CJ, Johnston RL (2014) A theoretical study of the structures and optical spectra of helical copper-silver clusters. Phys Chem Chem Phys 16:21039–21048. https://doi.org/10.1039/c3cp55507k
24. T. Lu, F. Chen, (2012) J. Comput. Chem., 33: 580–592
25. P. Debye - The Dipole Moment and Chemical Structure-Blackie and Son, London (1931).pdf
26. Corminboeuf C, Heine T, Weber J (2003) Evaluation of aromaticity: A new dissected NICS model based on canonical orbitals. Phys Chem Chem Phys 5:246–251. https://doi.org/10.1039/b209674a
27. Schleyer PVR, Maerker C, Dransfeld A, et al (1996) Nucleus-independent chemical shifts: A simple and efficient aromaticity probe. J Am Chem Soc 118:6317–6318. https://doi.org/10.1021/ja960582d
28. Poater J, Duran M, Sola M, Silvi B (2006) Theoretical evaluation of electronic localization in aromatic molecules by means of AIM and ELF topological approaches. Chem Rev 105:3911. https://doi.org/10.1021/cr030085x

Figures

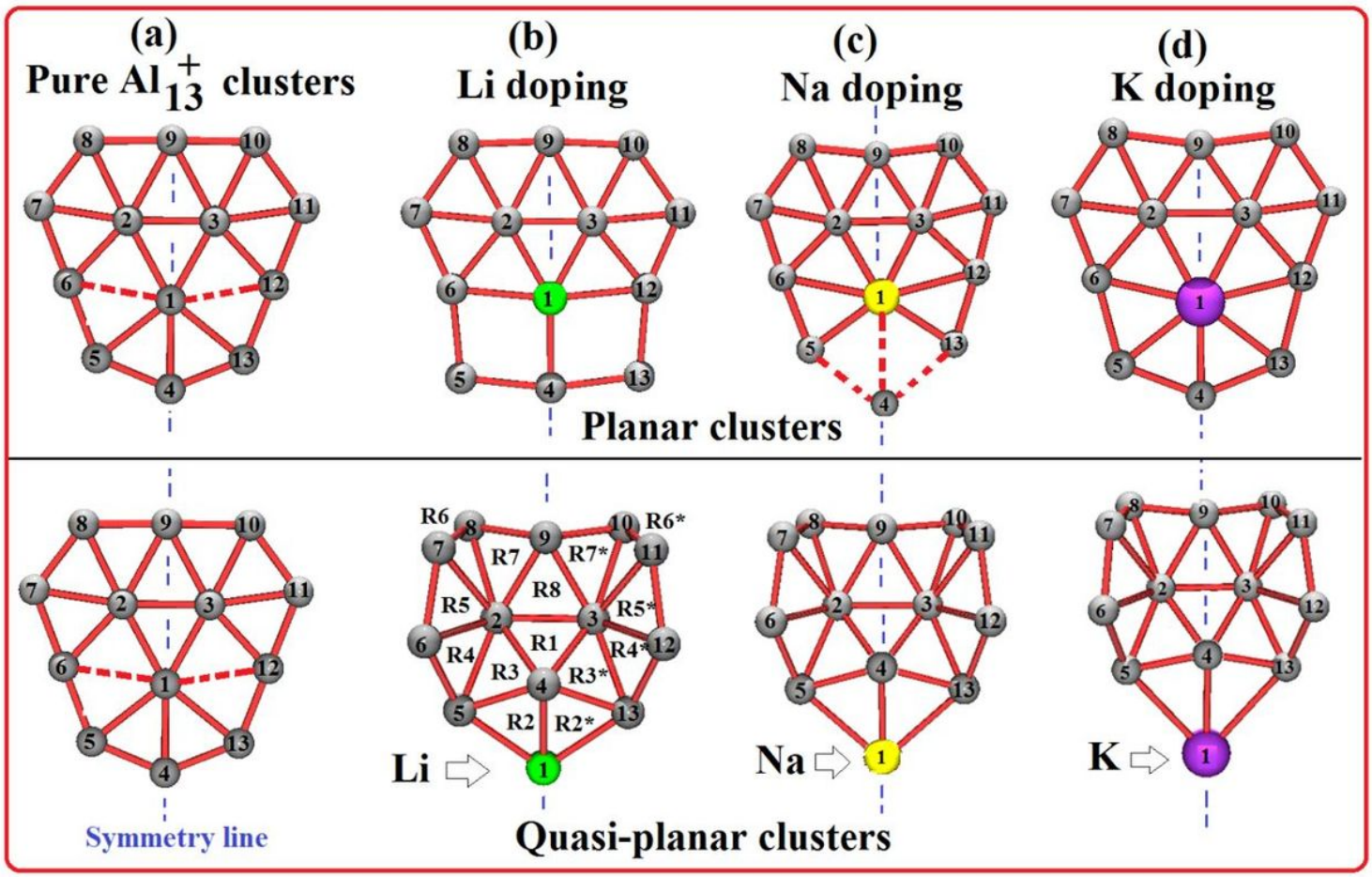

Figure 1

Optimized geometries of alkali atom doped planar and quasi-planar (Al12X)+ (X = Li, Na and K) clusters along with pure planar and quasi-planar Al13+ cluster. R2, R2*, R3, R3* etc. are symmetry related triangular rings on the cluster surface.

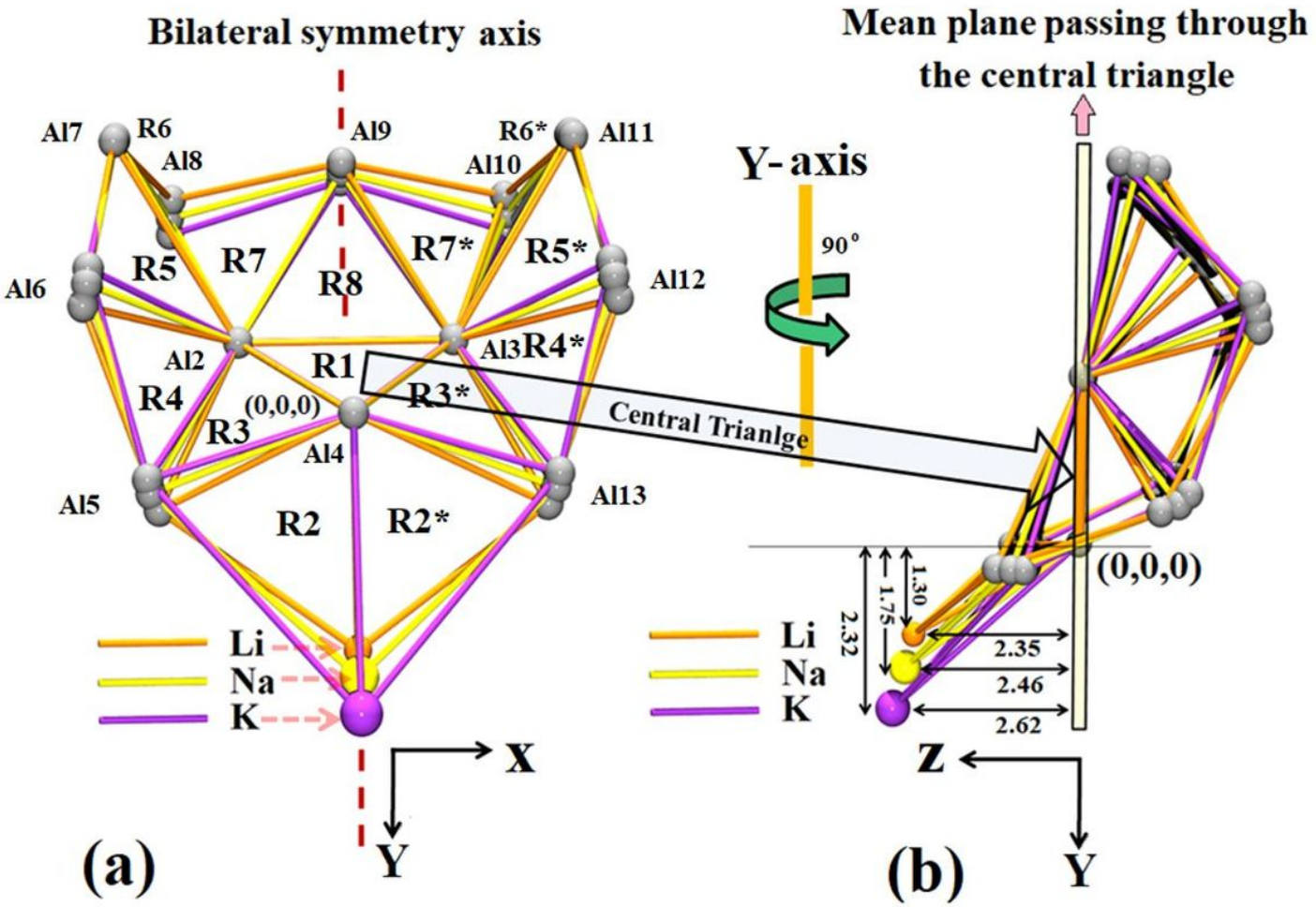

Figure 2

Superposed view of three alkali doped clusters. (a) Front view (b) Edge view (90° rotated around the symmetry line). Distance labels on the right hand panel are in Å unit.

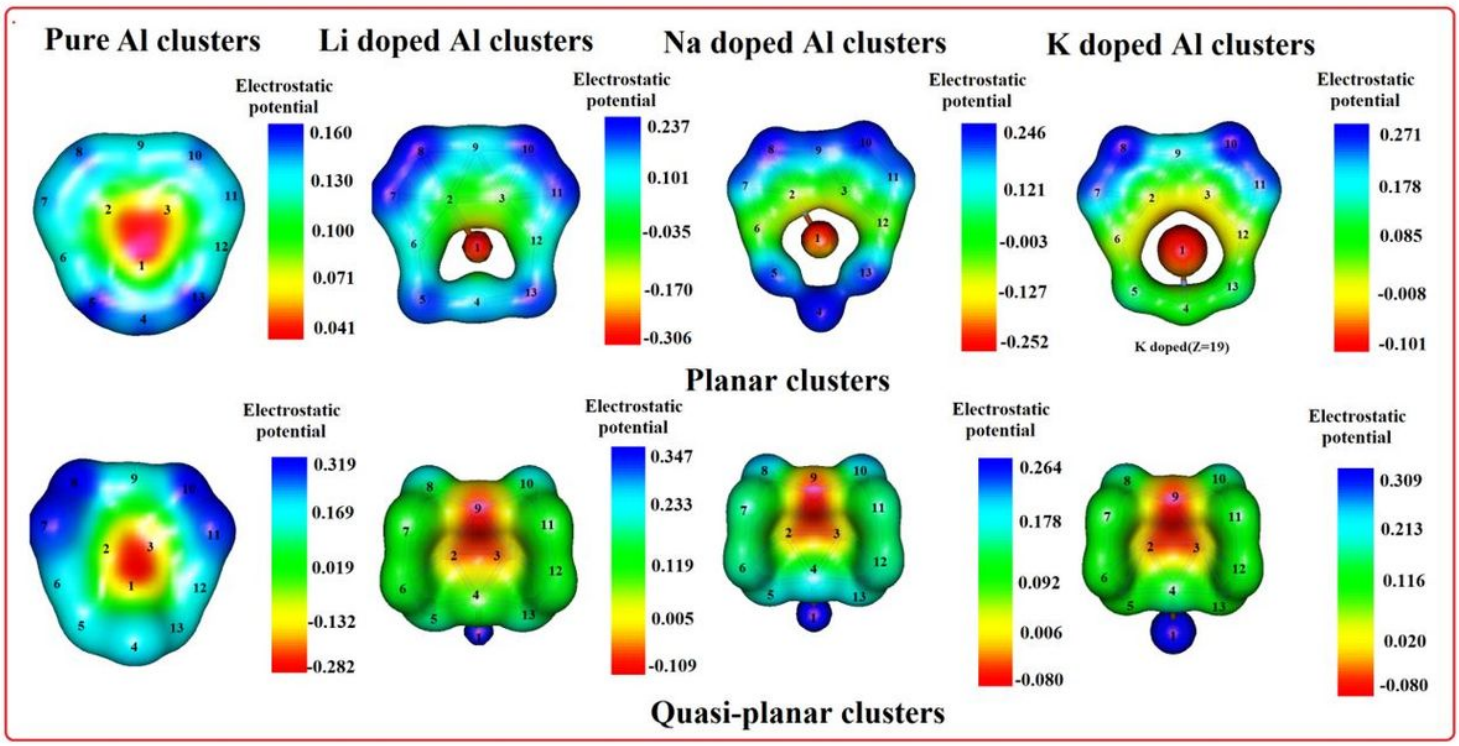

Figure 3

Electrostatic potential energy surfaces of planar and quasi-planar Al13+ clusters and the alkali (Li, Na and K) doped Al13+ clusters.

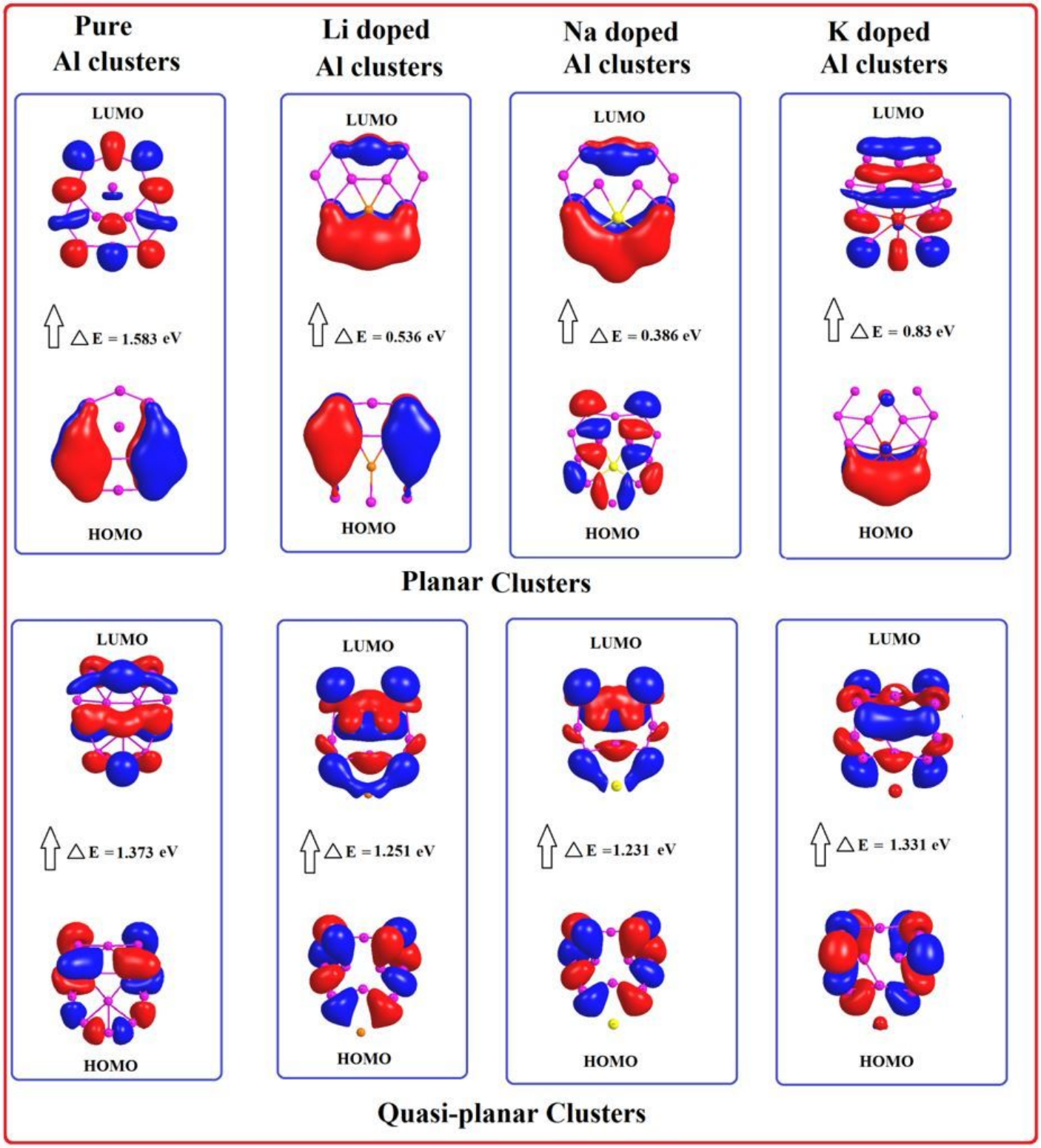

Figure 4

HOMO, LUMO orbitals and the HOMO-LUMO energy gap of the Li, Na and K doped clusters.

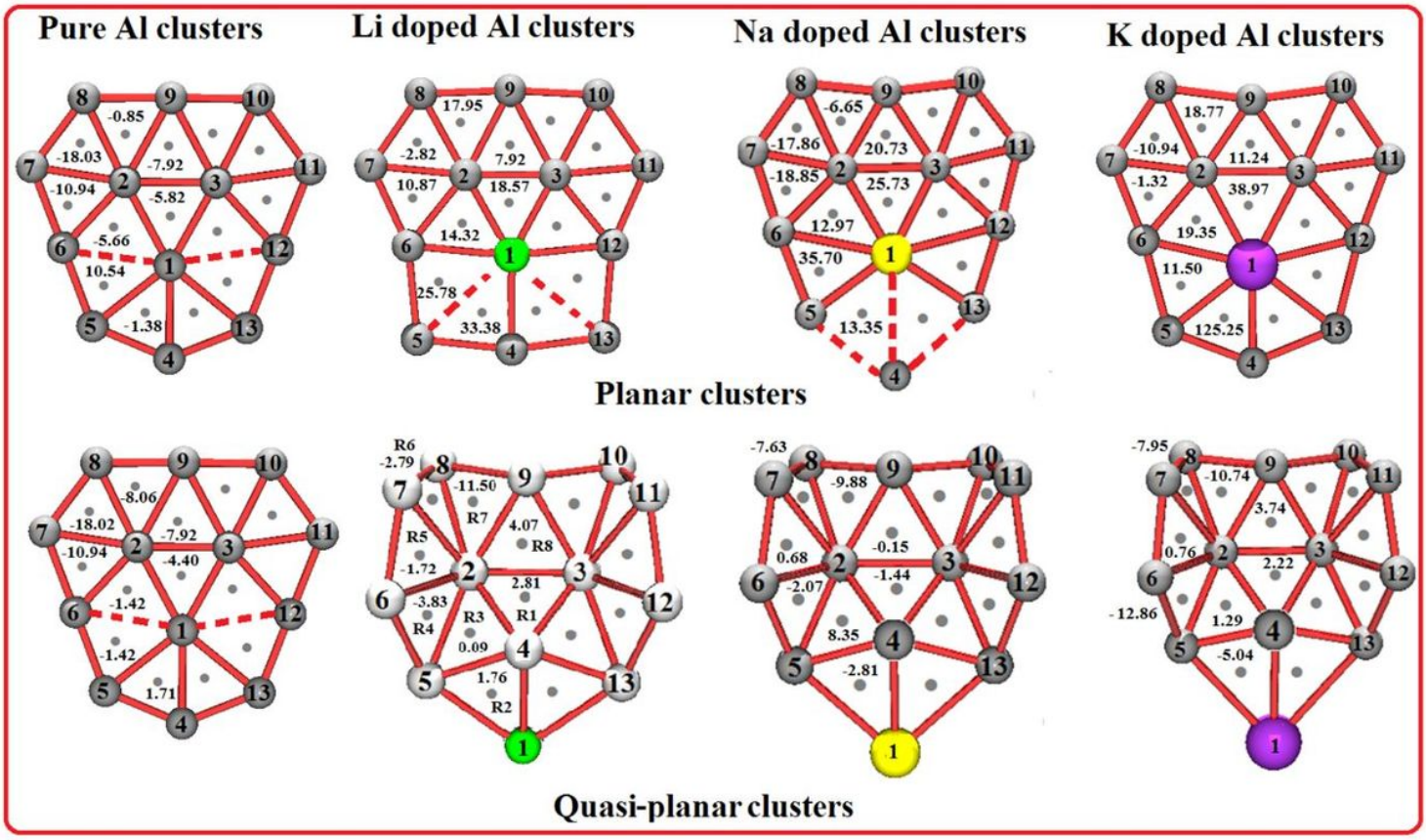

Figure 5

NICS(0) values (in ppm) at the ring centroids of the pure as well as alkali doped (Li, Na and K) clusters.

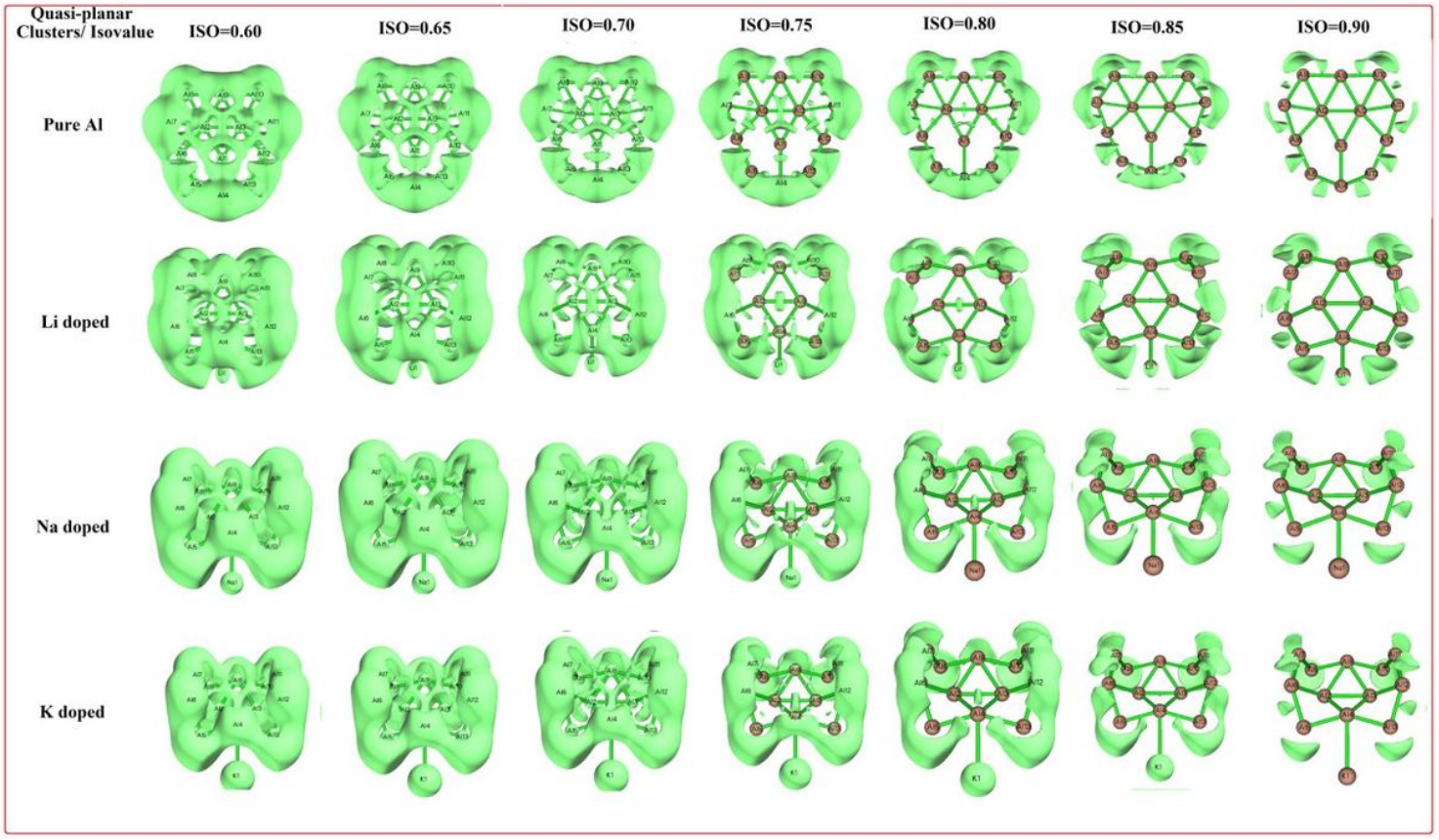

Figure 6

ELF surface of quasi-planar true minima Li, Na and K doped Al13+ cluster with pure Al13+ cluster.

Supplementary Files

This is a list of supplementary files associated with this preprint. Click to download.

- 20210215GA.docx
- 20210215SupplementaryMaterial.docx